

Nanoparticle plasma ejected directly from solid copper by localized microwaves

E. Jerby,^{1,a)} A. Golts,¹ Y. Shamir,¹ S. Wonde,¹ J. B. A. Mitchell,² J. L. LeGarrec,² T. Narayanan,³ M. Sztucki,³ D. Ashkenazi,¹ Z. Barkay,⁴ and N. Eliaz¹

¹Faculty of Engineering, Tel Aviv University, Ramat Aviv 69978, Israel

²IPR., U.M.R. No. 6251 du C.N.R.S., Université de Rennes I, 35042 Rennes, France

³European Synchrotron Radiation Facility, BP-220, 38043 Grenoble, France

⁴Wolfson Applied Materials Research Center, Tel Aviv University, Ramat-Aviv 69978, Israel

(Received 11 September 2009; accepted 19 October 2009; published online 9 November 2009)

A plasma column ejected directly from solid copper by localized microwaves is studied. The effect stems from an induced hotspot that melts and emits ionized copper vapors as a confined fire column. Nanoparticles of ~ 20 – 120 nm size were revealed in the ejected column by *in situ* small-angle x-ray scattering. Optical spectroscopy confirmed the dominance of copper particles in the plasma column originating directly from the copper substrate. Nano- and macroparticles of copper were verified also by *ex situ* scanning electron microscopy. The direct conversion of solid metals to nanoparticles is demonstrated and various applications are proposed. © 2009 American Institute of Physics. [doi:10.1063/1.3259781]

The phenomenon of fireball ejection to the atmosphere from solid dielectrics irradiated by localized microwaves has been presented recently.¹ Further studies showed that similar plasma balls can be generated from a wide range of solid or liquid substrate materials, such as silicon, germanium, ceramics, as well as pure and salty water.² Optical spectral measurements have revealed the dominance of the substrate materials in the light emitted from these fireballs (e.g., sodium light at 589 nm emitted from a fireball generated from a NaCl solution³). The small-angle x-ray scattering (SAXS) method, using synchrotron radiation, has been applied to study fireballs of this type. The first SAXS study of atmospheric-like fireballs⁴ presented analyses of the particle size distribution, density, and decay rate of fireballs made from borosilicate glass substrates. The results showed that these fireballs contained particles with diameters of ~ 50 nm and average number densities of $\sim 5 \times 10^9$ cm⁻³. Hence, it was suggested that these fireballs can be considered as a form of dusty plasma⁵ consisting of ensembles of charged nanoparticles in the plasma volume.

The present study applies the same localized microwave experimental technique⁶ to metallic, rather than dielectric, substrates. It is shown here that the molten hotspot induced in the solid copper substrate by the localized microwaves emits a confined plasma in the form of a fire column, and that this plasma contains copper nanoparticles. The experimental analyses employed in this study include *in situ* SAXS and optical spectroscopy of the ejected plasma column, and *ex situ* scanning electron microscopy of the collected particles in order to identify the composition and size of the nanoparticles created.

Copper nanoparticles feature useful physical properties⁷ and biomedical compatibility. They have been studied in various aspects⁸ and for different applications.^{9–13} Copper and copper-oxide nanoparticles can be produced by various means including plasmas.^{14–18} Microwaves or radio-

frequency generated plasmas have been used indirectly by employing other gases or reducing agents for the copper nanoparticles synthesis.¹⁹ Microwave plasmas were used to synthesize nanopowders of silver,²⁰ vanadium pentoxide, and zinc oxide²¹ from powder and granular precursors. Direct conversion of solid aluminum to nanoparticles and carbon nanotube synthesis were demonstrated in vacuum by femto-second pulsed lasers.^{22,23}

The experimental microwave setup used here for plasma ejection and direct conversion of solid metals to nanoparticles is depicted in Fig. 1. It consists of a rectangular waveguide (96×46 mm² inner cross section) with windows made of metallic vanes under cutoff to enable a direct view into the fire column (for observation, optical spectroscopy and x-ray scattering). The microwave cavity is energized by a 2.45 GHz magnetron providing an adjustable input power in the range of 0–1 kW. The movable inner electrode, made of copper or tungsten, enables the intentional excitation of a hotspot when brought in contact with the upper edge of a metal plate (the *emitter*), hence stimulating the fire column to be emitted in a controlled fashion. The emitter is made of 99.9% pure copper plate. Its dimensions are $20 \times 10 \times 1$ mm³ in the orientation shown in Fig. 1.

A stable plasma column, ejected from the upper edge of the copper emitter plate placed vertically on the floor of the

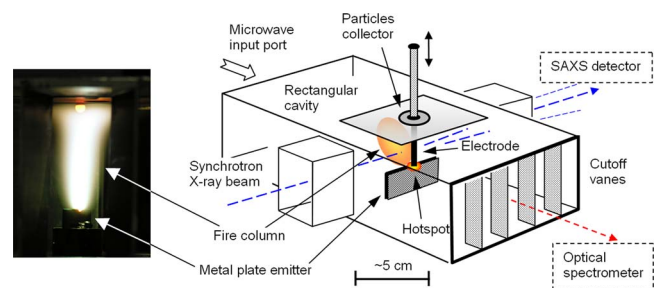


FIG. 1. (Color online) The experimental scheme of the microwave-generated copper plasma (right) and the plasma column ejected from the copper emitter to the collector in the microwave cavity (left).

^{a)}Author to whom correspondence should be addressed. Electronic mail: jerby@eng.tau.ac.il.

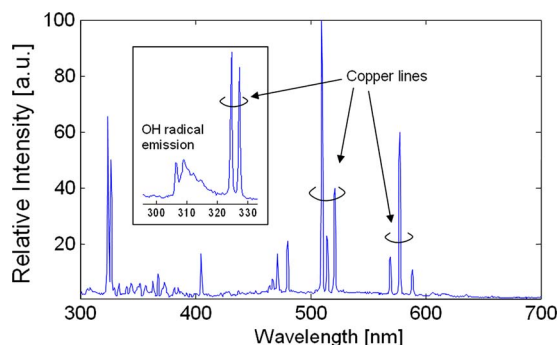


FIG. 2. (Color online) The optical spectrum of the copper plasma column. The inset shows the spectrum of the plasma column in the near-UV range.

cavity, is shown in the inset of Fig. 1. The plasma column jets toward the collecting plate installed on the cavity's ceiling (the *collector*). It remains stable and well confined as long as a microwave effective power in the range of 0.6–1.0 kW is supplied (typically for >1 min). The optical spectrum of the light emitted from the fire column is associated mostly with copper. Figure 2 shows a typical spectrogram obtained using an AvaSpec 3648 spectrometer. The spectral lines of copper in the visible range, at 578, 522, 511, and 515 nm, and in the near-UV range, at 327 and 325 nm, are clearly seen in this spectrogram, indicating the dominance of copper vapor in the plasma column. The UV range, shown in more detail in the inset of Fig. 2, also reveals the emission of an OH-radical spectral emission band around 310 nm. This resembles the spectrum of a fireball generated in a similar setup from tap or pure water³ instead of the copper emitter. The form of the OH-radical emission band obtained in the water-originating plasma experiments serves as an evidence for the local thermal equilibrium (LTE) condition here.²⁴ Hence, LTE can be speculated also for the copper plasma with the OH provided by the surrounding air. Under the LTE assumption, the Boltzmann plot method²⁵ applied to the spectra measured in this experiment results in electron temperatures of $(\sim 3\text{--}4) \times 10^3$ K, depending on the microwave effective power.

A typical SAXS pattern recorded from a copper fire column is shown in Fig. 3. These measurements were performed at the European Synchrotron Radiation Facility (ESRF), and the data were analyzed using the IRENA SAXS analysis package.²⁶ As in Ref. 4, the SAXS data was analyzed using the unified scattering function (USF) (Ref. 27) which indicated the presence of particles with radii of gyration of about 20 nm and 120 nm. The particle volume distribution was obtained by taking the inverse Fourier transform²⁶ of the scattered x-ray intensity versus the scattering vector, $q = (4\pi/\lambda)\sin(\theta/2)$, where θ and λ are the scattering angle and the x-ray wavelength, respectively. The resulting particle volume distribution is shown as an inset in Fig. 3. Three groups of particle size are seen here, around 27, 65, and 110 nm, which indicate the broad distribution of primary particles formed at different temperature zones within the fire column, their aggregates and agglomerates, respectively. The SAXS analysis shows also that the small particles have a solid surface while the larger particles have a more fractal structure (with power law exponents of 4.0 and 2.3, respectively) as in the case of flame grown particles.²⁷ The number densities are in the order of

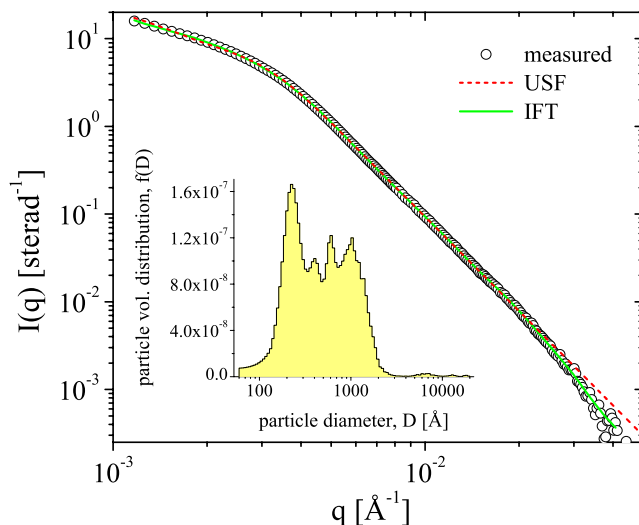


FIG. 3. (Color online) Typical SAXS intensity from the fire column and their analysis in terms of USF vs the scattering vector q . The particle size distribution within the copper fire column, computed by inverse Fourier transform, is shown in the inset (with peaks at 27, 65, and 110 nm).

$\sim 10^8$ cm⁻³ for the small particles and $\sim 10^6$ cm⁻³ for the aggregated particles.

The surface morphologies of the particles accumulated on the cavity's ceiling collector were characterized *ex situ* by the FEI Quanta 200FEG environmental scanning electron microscope (ESEM) operating in high-vacuum mode, using the Everhart-Thonley secondary electron detector. Several zones containing particles with different scales, shapes, and surface morphologies were identified in the collector specimens. Among them are mainly sea-urchin-like spheres (shown in Fig. 4) and sponge-like morphologies, in addition to nanospheres, nanowires, and nanotube shapes. Similar structures were also identified on the emitter surface, in addition to molten amorphous copper regions (similar to cathode spots). Circular arrays of particles were observed on the circumferences of concentric circles in various diameters ranging from millimeters down to micrometers. Figure 4

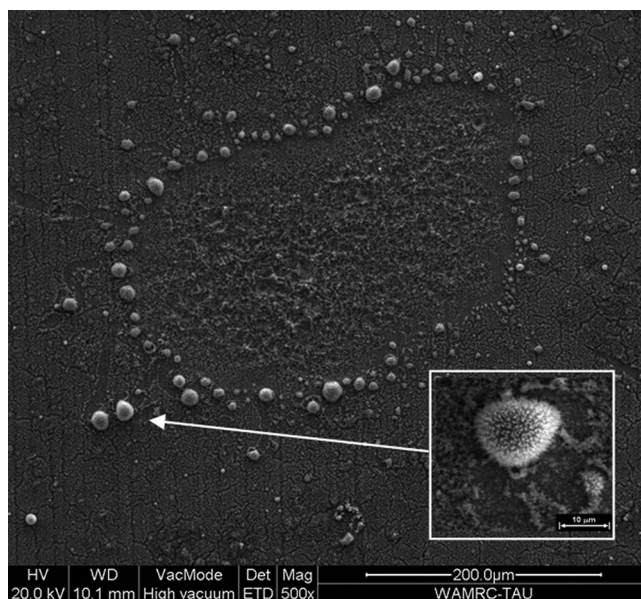


FIG. 4. Sea-urchin-like copper clusters and their circular arrangement observed on the collector surface *ex situ* by an ESEM.

shows a collector area covered with copper sea-urchin-like spheres organized on the surface in a circle. Higher-magnification images revealed that the sea-urchin-like spheres shown in the inset of Fig. 4 consist of smaller nanostructures of similar shapes (a resemblance is noted to the sea-urchin-like CuO microspheres synthesized in Ref. 17 by a hydrothermal microwave route in the presence of polyethylene glycol and NH_4OH). The chemical element composition was analyzed in ESEM by energy dispersive spectroscopy using a Si(Li) liquid nitrogen cooled Oxford x-ray detector. The analysis of different areas of the collector specimens showed that the sea-urchin-like spheres consist mainly of copper or copper oxide, with some impurities of W, Zn, Fe, Cl, and Ca attributed to the tungsten electrode.

Size measurements performed on the various particles in the different areas of the collector specimens showed that the outer dimension of the sea-urchin-like particles ranges between 1 and 10 μm , but their substructure dimension is of the order of 0.3 μm and even smaller; mostly in the range of 10–50 nm. The sizes of the sponge-like and spherical particles measured with a Molecular Imaging's PicoSPM atomic force microscope were found to be in the range of ~20–50 nm. These particle dimensions and structures observed *ex situ* coincide with the size distributions obtained *in situ* by SAXS.

This study shows that copper-vapor plasma can be generated directly and continuously from a solid copper surface in an air atmosphere using microwave radiation. The dusty plasma obtained consists of copper nanoparticles that tend to agglomerate in spherical structures such as the sea-urchin-like shapes shown above. These results may lead to the development of relatively simple techniques for metal plasma generation and nanoparticles synthesis directly from solid metals. The main advantage of the proposed approach, compared to other microwave-powered processes for making metallic nanoparticles (e.g., Refs. 20 and 21), is its simplicity resulting from the direct microwave application to solid metallic bulk rather than to presynthesized powder or metallic-salt solution. Other practical applications of this concept, such as sputtering, coating, microwave-excited metal-vapor lasers, and microwave-induced breakdown spectroscopy, can be conceived as well. The bulk modification effect observed may also enable microwave-induced variations of roughness and wettability. Further studies show that similar plasma columns can be ejected by this technique from other solid metals, e.g., aluminum or iron; hence, the phenomenon presented here and its potential applications can be generalized to microwave interactions with other metals as well.

The authors acknowledge the support by the European Synchrotron Radiation Facility (ESRF) and the Israeli Academy of Science (Grant No. 1270-04).

- ¹V. Dikhtyar and E. Jerby, *Phys. Rev. Lett.* **96**, 045002 (2006).
- ²E. Jerby, A. Golts, Y. Shamir, V. Dikhtyar, J. B. A. Mitchell, J. L. LeGarrec, T. Narayanan, M. Sztucki, N. Eliaz, D. Ashkenazi, and Z. Barkay, Proceedings of the Global Congress on Microwave Energy Applications (GCMEA-1), Otsu, Japan, 4–8 August, 2008 (unpublished), pp. 465–468.
- ³E. Jerby and V. Dikhtyar, in *Microwave Discharges: Fundamentals and Applications*, edited by Y. A. Lebedev (Yanus-K, Moscow, 2006), pp. 227–232.
- ⁴J. B. A. Mitchell, J. L. LeGarrec, M. Sztucki, T. Narayanan, V. Dikhtyar, and E. Jerby, *Phys. Rev. Lett.* **100**, 065001 (2008).
- ⁵V. N. Tsytovich, G. E. Morfill, and H. Thomas, *Plasma Phys. Rep.* **30**, 816 (2004).
- ⁶E. Jerby, V. Dikhtyar, O. Actushev, and U. Groszlick, *Science* **298**, 587 (2002).
- ⁷Y. Wang, M. Chen, F. Zhou, and E. Ma, *Nature (London)* **419**, 912 (2002).
- ⁸M. Samim, N. K. Kaushik, and A. Maitra, *Bull. Mater. Sci.* **30**, 535 (2007).
- ⁹J. A. Eastman, S. U. Cho, W. Yu, and L. J. Thompson, *Appl. Phys. Lett.* **78**, 718 (2001).
- ¹⁰J. A. Rodríguez, P. Liu, J. Hrbek, J. Evans, and M. Perez, *Angew. Chem., Int. Ed.* **46**, 1329 (2007).
- ¹¹Y. Lee, J. Choi, K. J. Lee, N. E. Stott, and D. Kim, *Nanotechnology* **19**, 415604 (2008).
- ¹²X. Kang, Z. Mai, X. Zou, P. Cai, and J. Mo, *Anal. Biochem.* **363**, 143 (2007).
- ¹³A. Esteban-Cubillo, C. Pecharroman, E. Agilar, J. Santaren, and J. Moya, *J. Mater. Sci.* **41**, 5208 (2006).
- ¹⁴W. Hu, M. Matsumura, K. Furukawa, and K. Torimitsu, *J. Phys. Chem. B* **108**, 13116 (2004).
- ¹⁵E. Marino, T. Huijser, Y. Creighton, and A. van der Heijden, *Surf. Coat. Technol.* **201**, 9205 (2007).
- ¹⁶M. Salavati-Niasari and F. Davar, *Mater. Lett.* **63**, 441 (2009).
- ¹⁷D. Keyson, D. P. Volanti, L. S. Cavalcante, A. Z. Simões, J. A. Varela, and E. Longo, *Mater. Res. Bull.* **43**, 771 (2008).
- ¹⁸A. Lagashetty, V. Havanoor, S. Basavaraja, S. D. Balaji, and A. Venkataraman, *Sci. Technol. Adv. Mater.* **8**, 484 (2007).
- ¹⁹H. Zhu, C. Zhang, and Y. Yin, *J. Cryst. Growth* **270**, 722 (2004).
- ²⁰J. L. H. Chau, M.-K. Hsu, C.-C. Hsieh, and C.-C. Kao, *Mater. Lett.* **59**, 905 (2005).
- ²¹J. H. Kim, Y. C. Hong, and H. S. Uhm, *Surf. Coat. Technol.* **201**, 5114 (2007).
- ²²S. Eliezer, N. Eliaz, E. Grossman, D. Fisher, I. Gouzman, Z. Henis, S. Pecker, Y. Horovitz, M. Fraenkel, S. Maman, and Y. Lereah, *Phys. Rev. B* **69**, 144119 (2004).
- ²³S. Eliezer, N. Eliaz, E. Grossman, D. Fisher, I. Gouzman, Z. Henis, S. Pecker, Y. Horovitz, M. Fraenkel, S. Maman, V. Ezersky, and D. Eliezer, *Laser Part. Beams* **23**, 15 (2005).
- ²⁴D. A. Levin, C. O. Laux, and C. H. Kruger, *J. Quant. Spectrosc. Radiat. Transf.* **61**, 377 (1999).
- ²⁵F. O. Borges, G. H. Cavalcanti, and A. G. Trigueiros, *Braz. J. Phys.* **34**, 1673 (2004).
- ²⁶J. Ilavsky and P. R. Jemian, *J. Appl. Crystallogr.* **42**, 347 (2009).
- ²⁷M. Sztucki, T. Narayanan, and G. Beaucage, *J. Appl. Phys.* **101**, 114304 (2007).